# FAILURE CRITERIA FOR COMPOSITE SLABS SUBJECT TO EXTREME LOADING CONDITIONS

K.A. Cashell, A.Y. Elghazouli and B.A. Izzuddin

*Department of Civil and Environmental Engineering*
*Imperial College London, UK*

## KEYWORDS

Composite slabs, extreme loading, fire conditions, failure criteria, strain concentrations

## ABSTRACT

This paper is concerned with the ultimate behaviour of composite steel/concrete floor slabs under extreme loading situations, particularly those that occur during severe building fires. The study focuses on the failure state associated with rupture of the reinforcement in composite slab members which become lightly reinforced in a fire situation due to the early loss of the steel deck. An account of a series of large scale ambient tests, undertaken on full slab members, is presented in the paper. The experimental arrangements are described together with the details of the specimens. Complementary analytical studies, carried out to assess the salient factors influencing the failure of composite slab members are also summarised. The assessments utilise detailed numerical models which adopt novel finite element formulations including geometric and material nonlinearities, as well as simplified analytical models for the prediction of failure deformations and associated load levels. The results of this investigation offer detailed insights into the key factors that govern the ultimate behaviour of composite floor systems under extreme loading conditions, and provide simplified tools which are suitable for implementation in performance based design procedures.

## INTRODUCTION

The performance of buildings with composite steel/concrete floors under extreme loading conditions has been the subject of extensive research investigations in recent years, e.g. [1-6]. Particular attention has been given to structural fire response after it was observed during real fires (e.g the Broadgate and Basingstoke fires) that buildings with composite floors had an inherent resistance against failure greater than that accounted for in design. Moreover, large-scale fire tests were conducted in the UK by the Building Research Establishment (BRE) and Corus (formerly British Steel) on the full-scale eight-storey building at Cardington [1, 7]. The findings of these tests, coupled with other numerical and experimental studies [e.g. 2-6], have verified the important role played by the composite floor slab in carrying the

gravity loading within the fire compartment, even after the loss of strength in the supporting secondary steel beams due to elevated temperature. Although the slab exhibits significantly lower bending capacity, the development of tensile membrane action coupled with several sources of over-design leads to considerable fire resistance capabilities. To this end, progress in the development of improved design approaches needs to be based on detailed assessment of the behaviour of floor slabs, using reliable and realistic modelling approaches coupled with the application of appropriate failure criteria.

One of the most important failure criteria for composite slabs is that related to rupture of the reinforcement. Under fire conditions, in addition to the possible failure of unprotected secondary steel beams, the thin steel deck within a composite slab incurs high temperature and becomes largely ineffective at an early stage. Thus, the slab behaves primarily as a concrete element with light mesh reinforcement which can experience large deflections thereby enabling the development of tensile membrane action. Prediction of the displacement and load levels corresponding to the fracture of the reinforcement is however a complex issue that necessitates a detailed treatment of the interaction between the concrete material and steel reinforcement, with due account of the appropriate loading and boundary conditions. Due to the uncertainties involved in various important material and response parameters, this problem also requires experimental validation and calibration.

This paper provides an overview of recent studies carried out to examine the performance of floor slabs. A series of idealised ambient slab tests are described, including the experimental set-up, specimen details and key results and observations. Particular emphasis is given to identifying and assessing the salient parameters with a view to investigating the appropriate failure criteria. Although the experiments described herein were conducted at ambient temperature, this is believed to be a significant step and essential precursor towards quantifying the elevated temperature behaviour, as well as the response under other extreme loading conditions. In addition, the main focus in this paper is on the response of simply-supported flat slabs, although the wider test programme has included tests on both one- and two-way spanning elements, with various restraint conditions and cross-sectional properties; the results of these can be found elsewhere [8].

After describing the experimental arrangement and discussing the main test results, the paper discusses the analytical procedures which have been developed to further investigate the response. These include a simplified analytical model which can represent the member response up to failure, and also more complex nonlinear finite element simulations. Importantly, the comparative assessments enable the calibration of realistic levels of idealised bond properties that can be used in analytical models for predicting the ultimate response. Although the work presented in this paper is restricted to simply-supported slabs without axial or rotational restraint, it accounts for the influence of key material and geometric parameters and can be readily adjusted to account for other structural and loading configurations.

**EXPERIMENTAL PROGRAMME**

A large number of ambient tests have been conducted on two-way spanning reinforced concrete slabs (out of which only eight tests are discussed herein) with a view to (i) gaining a greater understanding of the mechanisms dominating ultimate behaviour; (ii) assessing and quantifying the key parameters influencing behaviour; and (iii) establishing the appropriate failure criteria. A description of the testing arrangement is included herein together with the details of the materials and specimens examined.

*Testing arrangement*

The experiments were conducted in a purpose-built testing arrangement consisting of four large steel sections which were of sufficient strength and stiffness to resist the applied loads. A schematic of the testing arrangement is presented in Fig. 1. The steel sections were positioned on four large concrete

blocks at each corner and these were, in turn, fixed to the laboratory strong floor. The slabs were free to move both axially and rotationally at the edges and the arrangement could be readily modified to accommodate either rectangular or square members by adjusting two of the steel beams. Due to the nature of the behaviour, involving significant membrane action, a high-precision large-stroke actuator, operating in displacement-control, was utilised. Load was applied to the slab through 12 widely-spaced points, through a system of hinges attached to the actuator, in order to simulate distributed loading. Careful consideration was given to ensuring that an equal load was applied at each of the twelve points and also that the application remained vertical for the duration of the experiment. As a result, a system of square hollow sections, steel plates and ball joints was configured. The maximum vertical deflection in the centre of the slab was measured using a displacement transducer.
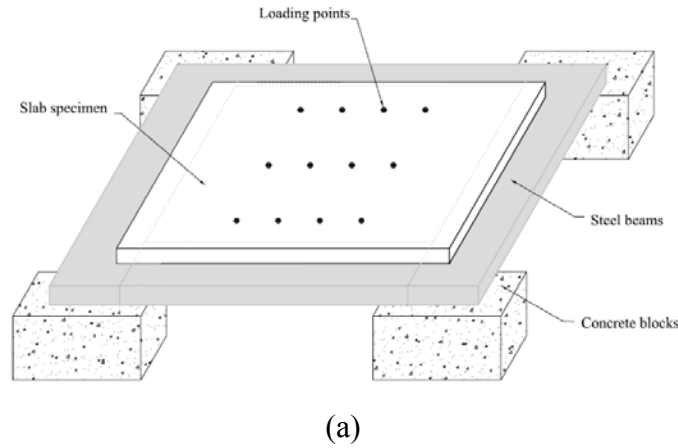


(a)

Figure 1: Experimental arrangement of slab tests

## Specimen details

This paper discusses the results of eight selected slab tests which included specimens with various geometric and material properties. As mentioned previously, these tests formed part of a wider test programme, the details of which can be found elsewhere [8]. The ultimate behaviour is particularly sensitive to several reinforcement characteristics, such as those related to the reinforcement ratio and the development of bond strength; accordingly, several tests were designed to examine these effects. To this end, the bond strength was inherently varied within the test programme by utilising both typical deformed bars (D6) and also welded mesh reinforcement (M6), thus providing a realistic assessment of the prevalent characteristics. Both reinforcement types had similar values of yield and ultimate strength which were approximately 550 and 600 $N/mm^2$, respectively. On the other hand, the ultimate strain exhibited by the reinforcement at fracture varied from 2.5% for M6 to 4% for D6. Careful attention was given to using equipment that can provide the full stress-strain relationship of the reinforcement bars up to fracture, as the actual shape of the curve can have a significant influence on the behaviour. For the concrete, an average compressive strength of about 40 $N/mm^2$ was considered in each of the tests.

Table 1: Slab test details

| Test | $L_1$ (mm) | $L_2$ (mm) | $h$ (mm) | Bar Type | $\rho_1$ (%) | $\rho_2$ (%) | $F_u$ (kN) | $F_{f,test}$ (kN) | $U_{f,test}$ (mm) |
|------|------|------|------|------|------|------|------|------|------|
| S1 | 2250 | 1500 | 40 | D6 | 0.35 | 0.35 | 32.3 | 56.6 | 90 |
| S2 | 2250 | 1500 | 60 | D6 | 0.24 | 0.48 | 48.4 | 104.5 | 84 |
| S3 | 2250 | 1500 | 60 | D6 | 0.24 | 0.24 | 40.4 | 72.5 | 76 |
| S4 | 1500 | 1500 | 60 | D6 | 0.24 | 0.24 | 51.3 | 87.6 | 68 |
| S5 | 1500 | 1500 | 60 | D6 | 0.52 | 0.52 | 108.8 | 167.5 | 63 |
| S6 | 2250 | 1500 | 60 | M6 | 0.24 | 0.24 | 46.3 | 71.1 | 69 |
| S7 | 2250 | 1500 | 60 | M6 | 0.24 | 0.24 | 48.6 | 82.2 | 64 |
| S8 | 1500 | 1500 | 60 | M6 | 0.24 | 0.24 | 46.3 | 78.3 | 74 |

Table 1 provides the relevant geometric and material properties pertaining to each slab, including the length of the long and short spans ($L_1$ and $L_2$, respectively), the depth ($h$) and also the reinforcement ratio in the long and short spans ($\rho_1$ and $\rho_2$). In order to provide a realistic insight into the bond and cracking behaviour, priority was given to employing realistic values of $h$ and $\rho$, as well as bar diameter ($\varphi$), although this resulted in comparatively low span/depth ratios owing to experimental constraints. In all specimens, the reinforcement was positioned at mid-depth of the section, with the longer bars placed at a greater effective depth than those across the short span.

*Test Results*

A large amount of data was obtained through the measurement of displacements, loads and strains in the tests. However, emphasis is placed herein on the deformation at failure of the specimens, which corresponds to fracture of the reinforcing bars. The overall load-displacement response obtained for S1 to S8 are given in Figs 2a and 2b below. In addition to the figures, the key experimental data relating to the failure load attained ($F_{f,test}$) and the corresponding failure displacement ($U_{f,test}$) is provided in Table 1. Also included in the table are the theoretical ultimate loads ($F_u$) according to classical yield line theory. All tests failed by fracture of the reinforcement across a localised through-depth crack. This type of failure was typically accompanied by a loud and distinctive noise, as well as a sudden drop in load.
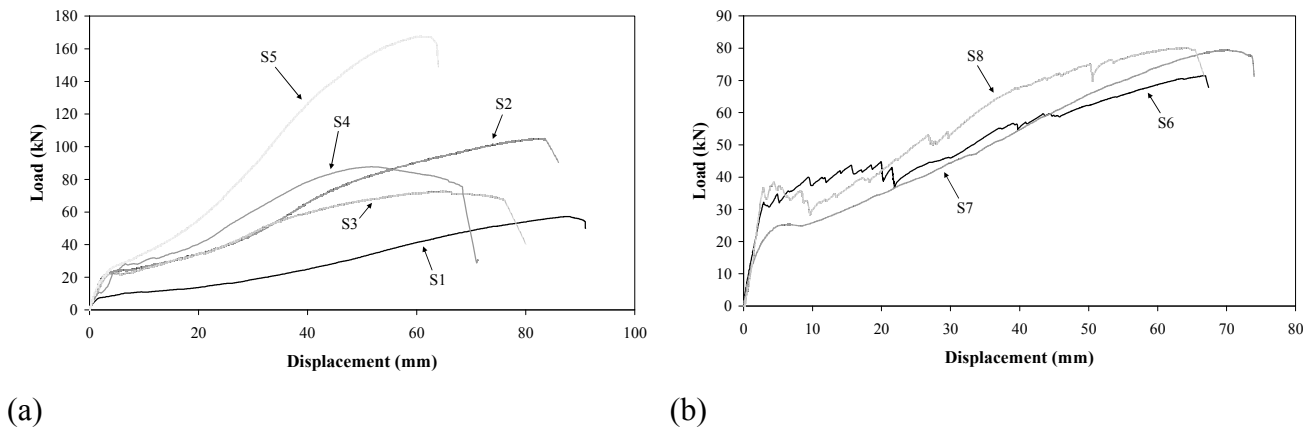


Figure 2: Load-displacement response for specimens with (a) D6 and (b) M6 reinforcement

Each slab surpassed the theoretical ultimate load, confirming the development of membrane action in all cases. The ratio of $F_{f,test}$ to $F_u$ varied between around 1.5 (Slab S6) and 2.2 (Slab S2). The scale of the load enhancement due to membrane action is directly related to the ductility of the reinforcement as low-ductility steel causes premature failure, thus preventing the large deflections necessary for significant tensile catenary action. The maximum load achieved was 167.5 kN in S5, which contained the greatest reinforcement ratio of all the tests whereas Slab S1 exhibited the lowest load-carrying capacity and failed at 56.6 kN. Analysis of the test results indicate that many factors influence the limiting levels of load and displacement that can be sustained by the slab. The load-carrying capacity and also the ability of the specimen to develop membrane forces is positively dependant on the type of reinforcement, the reinforcement ratio and the slab depth.. On the other hand, the failure displacement is directly related to the crack pattern that develops as greater cracking results in a lower concentration of strain in the reinforcement, thereby delaying failure. In this respect, $U_{f,test}$ was shown to be directly proportional to the reinforcement ductility, the reinforcement ratio (as this effects the level of cracking) and also the aspect ratio. However, failure is expedited for relatively deeper slabs. The results demonstrate that there are a number of inter-related parameters which influence the ultimate behaviour of floor slabs, hence necessitating in the development of realistic analytical procedures that can capture the influence of these key factors.

## ANALYTICAL MODELLING

The experimental results presented in the previous section furnished direct information on the relative influence of a number of geometric and material parameters on the ultimate response of simply supported floor slabs. In order to provide further insight into the behaviour, and to enable quantification of the response for the purpose of future design studies, there is a need for suitable analytical models that are validated and calibrated against experimental results and detailed numerical simulations. To this end, a simplified analytical model has been developed at Imperial College to predict the post-yield load-deflection response of floor slabs, as well as the level of deformation and load corresponding to failure, both at ambient and elevated temperature [9]. The approach provides a simple and realistic estimation of the ultimate conditions with due account of main geometric and material characteristics including the important influence of bond-slip. A detailed description of the procedure can be found elsewhere [9], but an outline of the key aspects and formulations are provided herein.

The model is developed building on an earlier one-dimensional simplified strip model [10, 11] and therefore assumes that the slab comprises a series of strip elements through the length and width of the element. The overall response is obtained by integrating the response of each strip (Fig. 3). It is assumed that cracks form in the locations predicted by conventional yield line theory and along the short span in the centre of the slab. The steel is assumed to have a rigid-hardening constitutive relationship defined by the yield strength $f_y$, ultimate strain $\varepsilon_u$ and hardening modulus $E_2$. On the other hand, the bond-slip relationship is idealised as a rigid-plastic relationship with a constant bond strength $\sigma_b$; this has been validated elsewhere [8]. Furthermore, the various parts of the slab, that are bounded by the full-depth cracks, are free to rotate both in-plane and out-of-plane in a rigid manner. Failure occurs by rupture of the reinforcement at mid-span in the short direction across the through-depth crack.
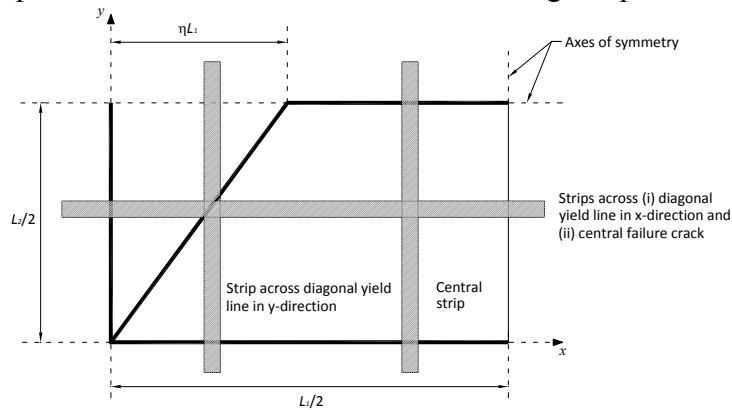


Figure 3: Quarter of the slab for formulation of simplified analytical model [9]

The width of each crack ($\Delta_s$) is calculated as a function of the vertical deflection ($U$) and then employed to obtain the total force in the steel across each crack ($T_s$). This is based on the bond strength that exists between the steel and the concrete and therefore accounts for strain concentration in the reinforcement. The total energy dissipated from the reinforcement as the slab deforms is determined as

$$\dot{D} = T_s \frac{d\Delta_s}{dU} \tag{1}$$

On the other hand, under a uniformly distributed load $q$, the total work done is equal to $q$ multiplied by the volume created by the slab as it deforms. Thus, the rate of external work performed by $q$ over the quarter slab is given by

$$\dot{E} = q \frac{L_1 L_2 (3 - 2\eta)}{24} \tag{2}$$

where $\eta$ is the yield line geometric parameter. Equilibrium is enforced by equating the rates of overall energy dissipation and the external work, enabling the determination of $q$ for a specific $U$. This leads to a

5

load-deflection relationship, which accounts for the development of stress concentrations within the reinforcement at crack locations and depends on the bond strength, material response of steel reinforcement, and crack widths as influenced by the slab deflection. Moreover, the level of load and deflection corresponding to rupture of the reinforcement can be obtained by assuming that the bond-slip length, $x_d$, is bounded by half the distance between the crack and the intersection of the yield lines

$$x_d = \frac{1}{2}\left(\frac{L_1}{2} - \eta L_1\right)$$ (3)

Thus, the predicted failure displacement ($U_{f,p}$) is obtained from either Eq. 4(a or b) according to

$$U_{f,p} = \sqrt{\frac{L_1}{2A_s E_2 \sigma_b}\left(T_u - T_y\right)} \qquad \text{if } x_d \geq \frac{T_u - T_y}{\sigma_b}$$ (4a)

$$U_{f,p} = \sqrt{\frac{L_1}{2A_s E_2 \sigma_b}\left(\left(T_u T_y + \sigma_b x_d\right)^2 - 2\sigma_b^2 x_d^2\right)} \qquad \text{if } x_d < \frac{T_u - T_y}{\sigma_b}$$ (4b)

where $A_s$ is the area of steel, and $T_u$ and $T_y$ are the ultimate and yield forces in the reinforcement.

Further verification of the load-displacement response was carried out through detailed finite element simulations using the advanced nonlinear analysis program ADAPTIC [12]. For brevity, a full description is not included herein but can be found elsewhere [8]. The program employs 2D shell elements [13,14] which combines computational efficiency with numerical accuracy and accounts for both geometric and material non-linearities. However, since the conventional smeared crack representation is used in the finite element models, they do not account for bond-slip hence cannot capture the strain concentration that occurs in the reinforcement across cracks. However, the finite element simulations can still provide valuable information regarding the behaviour of the floor slabs under extreme loading conditions [13,14], particularly in terms of the overall load-displacement response.

**COMPARITIVE ASSESSMENT**

This section compares the experimental results to the analytical predictions of both the simplified analytical model (hereafter referred to as the SAM) and the finite element model (denoted as the FEM). Two experiments (S1 and S8) are selected for detailed analysis of the load-deflection performance; these slabs incorporate both reinforcement types. The FEM analysis employs a mesh comprising $30 \times 20$ uniform-thickness shell elements, based on a mesh sensitivity assessment. On the other hand, the SAM is based on rigid-plastic hardening behaviour and hence the elastic and elasto-plastic displacements are not included. This procedure terminates upon either fracture of the reinforcement or crushing of the concrete and hence the final point on each curve represents failure. In addition to the SAM and FEM predictions, simulations from another analytical model, which has been developed by BRE [2,3], are also provided. This method assumes a similar crack pattern to the SAM and also ignores the elastic and elasto-plastic stages of the response. Unlike the SAM which is based on an assumed kinematic mode, the BRE approach is based on an assumed internal stress distribution.

The experimental load-deflection responses for S1 and S8 are presented in Figs 4a and 4b, respectively, together with the corresponding analytical simulations. It is evident that the FEM predicts the elastic response and cracking load reasonably well in both cases. The experimental responses generally exhibit greater strain hardening properties in the plastic range than is depicted by the model as the smeared-crack solution procedure cannot reliably assess the strain concentrations across cracks. Significant cracking occurred in both tests and, as a consequence, the bond-slip length and the length of reinforcement undergoing plastic deformation was greater than if less cracks had developed. In spite of this, the overall load-deflection response simulated by the FEM compares reasonably well with the test results. On the other hand, the initial load resistance predicted by the SAM corresponds to a value very close to the yield

line capacity ($F_u$ in Table 1). As the displacement increases further, the predicted behaviour correlates well with the experimental response in the plastic range. The prediction of maximum load capacity is almost identical to the actual behaviour. It is also evident that the BRE prediction provides a reasonable correlation with the experimental response. The SAM response is generally stiffer than the BRE proposal as it is based on an assumed kinematic mode rather than an internal stress distribution. In summary, the favourable comparisons provided through these examples demonstrate the reliability of the kinematic expressions and the corresponding load-deflection response characteristics of the proposed model.

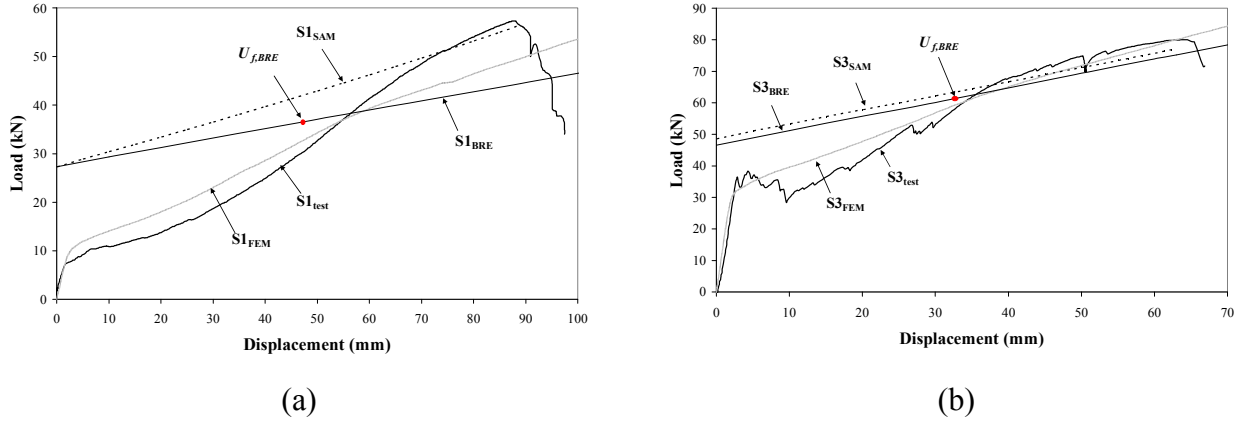|               (a)               |               (b)               |

Figure 4: Load-deflection response of (a) S1 and (b) S8

One of the most important aspects of the proposed SAM model is establishing the appropriate levels of load and displacement corresponding to failure. To this end, the failure displacements and loads obtained from the simplified analytical model ($U_{f,SAM}$ and $F_{f,SAM}$, respectively) are included in Table 2, together with the corresponding test values. Also included are the predicted failure displacements according to the BRE model, $U_{f,BRE}$.

Table 2: Failure analysis

| Test | Bar Type | $F_u$ (kN) | $F_{f,test}$ (kN) | $F_{f,SAM}$ (kN) | $U_{f,test}$ (mm) | $U_{f,SAM}$ (mm) | $U_{f,BRE}$ (mm) |
|------|----------|------------|-------------------|------------------|-------------------|------------------|------------------|
| S1 | D6 | 32.3 | 56.6 | 56.4 | 89.8 | 89.2 | 51 |
| S2 | D6 | 48.4 | 104.5 | 88.5 | 83.6 | 82.8 | 51 |
| S3 | D6 | 40.4 | 72.5 | 75.5 | 76.2 | 75.1 | 51 |
| S4 | D6 | 51.3 | 87.6 | 87.2 | 68.4 | 66.8 | 34 |
| S5 | D6 | 108.8 | 167.5 | 167.8 | 62.9 | 63.2 | 34 |
| S6 | M6 | 46.3 | 71.7 | 67.7 | 68.5 | 66.6 | 50 |
| S7 | M6 | 48.6 | 78.3 | 78.3 | 73.7 | 72.2 | 50 |
| S8 | M6 | 46.3 | 82.2 | 77.1 | 64.2 | 62.6 | 33 |

It is evident from Table 2 that the analytical predictions provide a reasonably accurate assessment of the experimental failure conditions. However, the results are clearly dependant on a realistic representation of the material properties, including the bond strength between steel and concrete. The test results therefore provide direct calibration of the idealized bond strength that needs to be employed in the model. As discussed previously, the bond-slip behaviour is idealised as a rigid-plastic relationship. On this basis, representative values of effective bond strength ($\sigma_b$) were determined to be in the range of 0.2-0.3N/mm$^2$ for D6 and 0.3-0.4N/mm$^2$ for M6. Clearly, due to the different loading and behavioural conditions, these values are considerably lower than those measured in conventional pull-out bond tests. It is also important to recall that minimum cracking is assumed in the analytical model; hence, the bond strength employed implicitly accounts for the resulting influence of any additional cracks that develop. In addition, whilst the BRE model is semi-empirical in its treatment of several key parameters, it seems to provide conservative predictions for typical ranges.

## CONCLUDING REMARKS

This paper described recent studies into the ultimate behaviour of composite floor slabs, including large-scale experimental testing as well as the development of a simplified analytical model. Particular emphasis was given to the failure condition associated with reinforcement fracture. The results demonstrated the reliability and accuracy of the proposed model. Importantly, the model enables a reliable prediction of the limiting levels of load and displacement which can be sustained. It captures the influence the key geometric and material parameters including the crucial influence on bond-slip. The work described herein is part of a wider experimental and analytical study, which has investigated the effects of other material, geometric, boundary and loading conditions.

## REFERENCES

[1] Wang, Y.C., Lennon, T., and Moore, D.B., "The behaviour of steel frames subject to fire", Journal of Constructional Steel Research, 35, 1995, pp. 291–322.

[2] Bailey, C.G. and Moore, D.B., "The structural behaviour of steel frames with composite floor slabs subject to fire. Part 1: Theory", The Structural Engineer, 78(11), 2000, pp. 19–27.

[3] Bailey, C.G. and Moore, D.B., "The structural behaviour of steel frames with composite floor slabs subject to fire. Part 2: Design", The Structural Engineer, 78(11), 2000, pp. 28-33.

[4] Gillie, M., Usmani, A.S., and Rotter, J.M., "A structural analysis of the first Cardington test", Journal of Constructional Steel Research, 57, 2001, pp. 581-601.

[5] Elghazouli, A. Y. and Izzuddin, B. A., "Analytical assessment of the structural performance of composite floors subject to compartment fires", Fire Safety Journal, 36, 2001, pp. 769–793.

[6] Lim, L., Buchanan, A. and Moss, P., "Experimental testing and numerical modelling of two-way concrete slabs under fire conditions", Journal of the Structural Engineering Society New Zealand, SESOC, 2003, pp.12-26.

[7] O'Connor, M. A., Kirby, B. R. and Martin, D. M., "Behaviour of a Multi-Storey Composite Steel Framed Building in Fire", The Structural Engineer, 81(2), 2003, pp. 27-36.

[8] Cashell, K.A., "Ultimate behaviour of floor slabs under extreme loading conditions", PhD Thesis, to be submitted to the University of London, 2009.

[9] Omer, E., Izzuddin, B.A., Elghazouli, A.Y., "Failure assessment of simply supported floor slabs under elevated temperature", Structural Engineering International, 16, 2006, pp.148 – 155.

[10] Izzuddin, B. A. and Elghazouli, A. Y., "Failure of lightly reinforced concrete members under fire. I: Analytical modelling", Journal of Structural Engineering, 130(1), 2004, pp. 3–17.

[11] Elghazouli, A. Y. and Izzuddin, B. A., "Failure of lightly reinforced concrete members under fire. II: Parametric studies and design considerations", Journal of Structural Engineering, 130(1), 2004, pp.18–31.

[12] Izzuddin, B. A. "Nonlinear dynamic analysis of framed structures", PhD thesis, Imperial College, University of London, 1991.

[13] Izzuddin, B. A., Tao, X. Y. and Elghazouli, A. Y., "Realistic modelling of composite and reinforced concrete floor slabs under extreme loading. I: Analytical method", Journal of Structural Engineering, ASCE, 130(12), 2004, pp.1972–1984.

[14] Elghazouli, A. Y. and Izzuddin, B. A., "Realistic modelling of composite and reinforced concrete floor slabs under extreme loading. II: Verification and application", Journal of Structural Engineering, ASCE 130(12), 2004, pp.1985–1996.